Mechanism of Solid/Liquid Interfacial Reactions. The Hydrolytic Dissolution of Solid Triphenylmethyl Chloride in Aqueous Solution

Kin Yip Tam,[†] Richard G. Compton,*[,†] John H. Atherton,[‡] Colin M. Brennan,[‡] and Robert Docherty[‡]

Contribution from the Physical and Theoretical Chemistry Laboratory, Oxford University, South Parks Road, Oxford OX1 3QZ, United Kingdom, and Zeneca Limited, PO Box 42, Blackley, Manchester M9 3DA, United Kingdom

Received August 21, 1995. Revised Manuscript Received February 12, 1996[⊗]

Abstract: The reaction between solid triphenylmethyl chloride (TPMCl) and water, TPMCl(s) + H_2O(l) → TPMOH-(aq) + H^+(aq) + Cl^-(aq), where TPMOH is triphenylmethyl alcohol, has been investigated using the channel flow cell method. It is found that hydrolysis proceeds via a direct heterogeneous fashion whereby the reaction occurs *at* the solid−liquid interface rather than in solution after the prior dissolution of TPMCl. Kinetic parameters are reported including the effect of ionic strength. Further, using experiments conducted with different surfaces of single crystals of TPMCl, it is shown that the rate of the interfacial process depends on the availability of exposed chlorine atoms in the reacting crystal plane. In situ atomic force microscopic studies indicate that the TPMCl surface, once in contact with water, is covered rapidly by a porous product layer. However, the latter provides a negligible effect on the reaction rate because of its high porosity.

Introduction

The fundamental study of reactions between solids and liquid phase species is the subject of rapidly growing attention.[1] One successful approach to the measurement of the interfacial kinetics of such processes involves the use of a channel flow cell (CFC).[2,3] The CFC comprises a rectangular duct through which solution is forced under laminar flow conditions and the solid substrate of interest is embedded smoothly in one wall of the flow cell (Figure 1). A suitable detector, which may be electrochemical or spectroscopic, is located immediately downstream of the solid surface so as to monitor either the release of products or alternatively the consumption of reactants. Since the reacting surface and the detector are linked via a well-defined hydrodynamic regime, the mass transport between the two may be calculated from a knowledge of the convection and diffusion in the cell. In this manner the separate contributions from mass transport and interfacial chemical phenomena to the response of the detector can be quantitatively assessed and the sought interfacial mechanism identified by measuring the detector signal as a function of solution flow rate over a suitably wide range of the latter. The technique is illustrated in Figure 1 and has been successfully applied to the study of the dissolution of benzoic acid[2] and to the reaction between solid cyanuric chloride and an aqueous solution of an aromatic amine.[3] In the former case it was demonstrated that the method could provide information about the kinetics of the interfacial dissolution process, unlike alternative techniques, such as the rotating disc method, where the interfacial region is saturated with the dissolving material and so the rate at which this appears in bulk solution simply reflects the rate of transport across the diffusion layer of the disc. The interfacial dissolution kinetics were shown to be very sensitive to the morphology of the dissolving solid.[2] In the latter case[3] the coupling reaction was found to take place in solution a thin layer—the "reaction layer"—adjacent to the dissolving solid but at an overall rate controlled by the rate at which the cyanuric chloride dissolved from the solid surface.

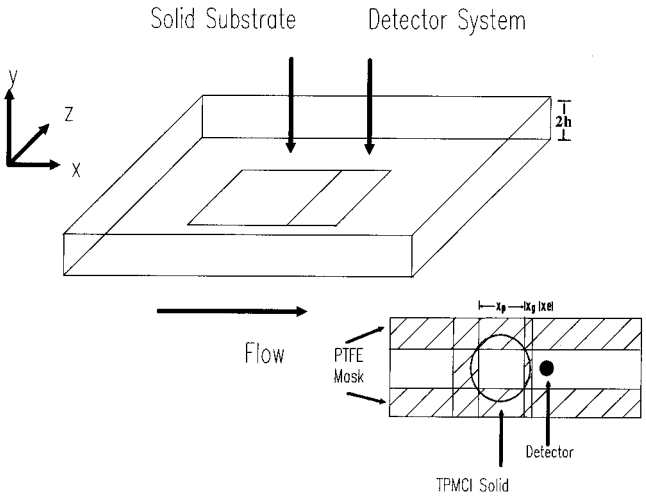

Figure 1. Schematic diagram of a channel flow cell. The inset shows a top view of the cover plate utilized in this work.

In this paper we apply the CFC method to study the dissolution and hydrolysis of solid triphenylmethyl chloride, TPMCl. While the homogeneous solvolysis of TPMCl in various solvents has been extensively studied from an early date[4,5] with the conclusion that the reaction follows a unimolecular nucleophilic substitution mechanism (Scheme 1), little, if any, work on the hydrolysis of solid TPMCl appears to have

* Author to whom any correspondence shoud be sent.
† Oxford University.
‡ Zeneca Limited.
⊗ Abstract published in *Advance ACS Abstracts,* April 15, 1996.

(1) Atherton, J. H. *Res. Chem. Kinet.* **1994**, *2*, 193.
(2) Compton, R. G.; Harding, M. S.; Pluck, M. R.; Atherton, J. H.; & Brennan, C. M. *J. Phys. Chem.* **1993**, *97*, 10416.
(3) Compton, R. G.; Harding, M. S.; Atherton, J. H.; Brennan, C. M.; *J. Phys. Chem.* **1993**, *97*, 4677.
(4) Hughes, E. D.; Ingold, C. K.; Mok, S. F.; Patai, S.; Pocker, Y. *J. Chem. Soc.* **1957**, 1265.
(5) Golomb, D. *J. Chem. Soc.*, **1959**, 1327.

S0002-7863(95)02914-3 CCC: $12.00

Scheme 1

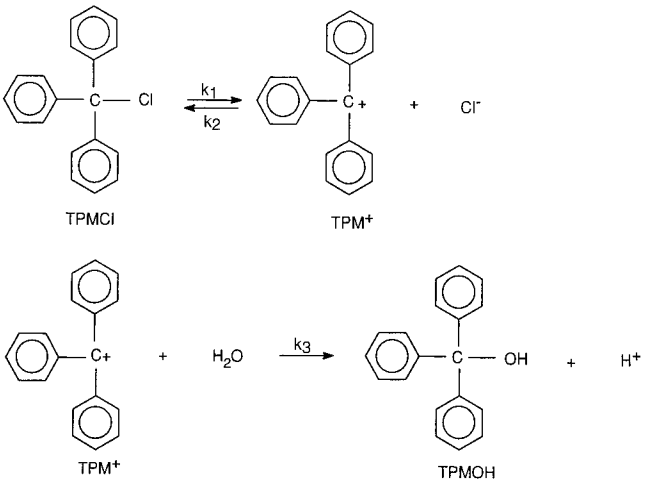

been undertaken. Work on the rate of hydrolysis of TPMCl in a two phase water−toluene system[6] shows that particular interfacial process to be exceptionally fast and it has been speculated[1] that the reaction may likely occur *at* the liquid−liquid interface. This observation combined with the recognition that the solubility of TPMCl in water is very low—ca. 10^{-8} M as predicted using an established correlation[7]—has led us to investigate the reaction of solid TPMCl with water to see if the hydrolysis to form TPMOH is authentically heterogeneous, occurring *at* the solid/liquid boundary, or if it proceeds via initial release of TPMCl from the reacting surface followed by hydrolysis in homogeneous bulk solution. Given the behavior in liquid−liquid systems,[4−6] TPMCl was selected as a likely candidate for genuine heterogeneous reaction.

In the present study, the CFC method is employed to investigate the hydrolysis of solid TPMCl using as substrates, namely, fused pellets, pellets pressed from particulate material, and single crystals. Both a chloride ion-selective electrode (ISE) and a conductivity detection system are separately employed for the sensitive monitoring of the release of the hydrolysis products in the CFC. The former is optimally employed at relatively high ionic strengths ($>10^{-2}$ M) and the latter in more dilute solutions ($<10^{-2}$ M) so that the two detection approaches between them cover the full range of salt concentrations.

The CFC kinetic results in conjunction with ex situ scanning electron micrographs and in situ atomic force micrographs of the reacted or reacting surface will be shown to allow the interfacial reaction mechanism to be unambiguously identified. Contrary to previous observations in the benzoic acid and cyanuric chloride systems (vide supra), the solid TPMCl hydrolysis will be shown to proceed directly *at* the reacting surface and its rate to be governed by the density of exposed chlorine atoms in any particular reacting crystal plane.

Experimental Section

A schematic diagram of the CFC is given in Figure 1. The cell is composed of a rectangular duct (about 4.5 cm long, 0.1 cm deep, and 0.6 cm wide) cut in a perspex block and closed by a cover plate. The solid substrate, either in the form of fused pellet, pressed pellet, or single crystal, was embedded into the cover plate together with a downstream detector system (vide infra) for the monitoring of the amount of product released. Solutions were made up using deionized water of resistivity $>10^7$ Ω. The ionic strength was adjusted to the desired value by adding AR grade potassium nitrate. Solution flow rates were obtained in the range 10^{-3}−10^{-1} cm^3 s^{-1} using gravity feed.[2,3] In every experiment, the temperature of the flow system was maintained at 25 + 0.5 °C using an air-thermostat.

The cover plate was a block of teflon or perspex with a circular hole (see Figure 1) which supported a pellet or single crystal. The solid substrate was masked with thin Teflon tape so that a known area of the solid was exposed to solution. The precise geometry of the assembled pellet/detector system was measured to +0.002 cm with a traveling microscope.

Commercially available TPMCl powder (Aldrich, 98%) was employed without further purification. For a fused pellet, the compound was directly melted in the Teflon block at 150 °C. Upon solidification, the surface of the pellet was cut flush to the cover plate surface. In the case of pressed pellet a pressure of 5.6×10^9 Nm^{-2} was generated by a screw press to compact the powdered material directly into the perspex block.[8] The particle size distribution of the TPMCl powder used to form pressed pellets was measured by a light scattering method (Zeneca, Huddersfield). Three different distributions were used, with the finer powders being obtained from the coarser by mechanical grinding. The distributions are characterized by the sizes corresponding to cumulative frequencies of 10% and 90%. These values for the three distributions used were (i) 14−90, (ii) 47−445, and (iii) 36−738 μm, respectively. In the subsequent discussions, the porosity of surface layers formed by compacting these separate powders is scrutinized. It is therefore appropriate to consider a volume average particle diameter, $D[4, 3]$, defined as $\Sigma nd^4/\Sigma nd^3$, where d indicates the diameter of individual particles of number n in the system. $D[4,3]$ for particles with distributions (i), (ii), and (iii) are 53.5, 278.2, and 332.4 μm, respectively.

For single crystal experiments it was noted that Kahr and Carter[9] reported that TPMCl could be grown into three different crystal forms. They prepared a trigonal polymorph ("Phase I" in their notation[9]) from toluene solution while two triclinic polymorphs (Phases II and III) were grown from pentane. In the present study, the slow cooling process[10−13] was implemented to grow a single triclinic form (Phase III). First a saturated solution was produced by adding TPMCl powder to 500 mL of anhydrous pentane (Aldrich, >99%) at 32 °C. The resulting solution was filtered twice and 0.5 mL of acetyl chloride added to the filtrate. Then the saturated solution was transferred to a 500 mL crystal growing flask. Seed crystals were added and the solution was kept in motion by a slowly rotating paddle to ensure a homogeneous TPMCl concentration over the crystal surface. The solution cooling rate was controlled by using a home-built programmable temperature water bath. It consisted of an electronic controlling system which triggered the illumination of a powerful light bulb (275 W IR reflector, GEC Electronics), which shone through one side of the water bath to provide heating. The rate of cooling was adjusted to 0.04 °C per hour from 32 to 20 °C. The crystals formed were approximately 0.5 × 0.5 × 0.5 cm in size. Figure 2 shows a typical crystal grown from this procedure. Suitably smaller sized crystals prepared in this way were characterized using X-ray diffraction techniques (Chemical Crystallography Laboratory, Oxford). The unit cell dimensions and the unit cell volume[14] are in excellent agreement with the Phase III triclinic form reported by Kahr and Carter.[9] Contact goniometry and a genetic algorithm-based matching procedure[15] were used to index large crystals. Different crystal faces—$(\bar{1}11)$, (010), and $(\bar{1}10)$—were employed for CFC experiments. To this end the crystal was embedded into cover plate using wax so that only a specific plane was exposed to the solution.

(6) Silhanek, J.; Kondradova, L.; Simeckova, O.; Horak, J. *Collect. Czech. Chem. Commun.* **1982**, *47*, 2904.

(7) Hansch, C.; Quinlan, J. E.; Lawrence, G. L. *J. Org. Chem.* **1968**, *33*, 347.

(8) Oberg, E.; Jones, F. D. *Machinery's Handbook*; 18th ed.; Industrial Press: New York, 1970.

(9) Kahr, B.; Carter, R. L. *Mol. Cryst. Liq. Cryst.* **1992**, *219*, 79.

(10) Brice, J. C. *The Growth of Crystals from Liquids*; North-Holland Publishing Co.: Amsterdam.

(11) Brice, J. C. *Crystal Growth Processes*; Blackie & Son Ltd.: Glasgow, 1986.

(12) Simon, B.; Boistelle, R. *J. Cryst. Growth* **1981**, *52*, 779.

(13) Tarjan, I.; Matrai, M. *Laboratory Manual on Crystal Growth*; Akademiai Kiado, Budapest.

(14) The unit cell dimenions derived in this work are as follows: a = 14.1506 Å, b = 21.3190 Å, c = 13.0559 Å, V = 3710 Å^3.

(15) Tam, K. Y.; Compton, R. G. *J. Appl. Cryst.* **1995**, *28*, 640.

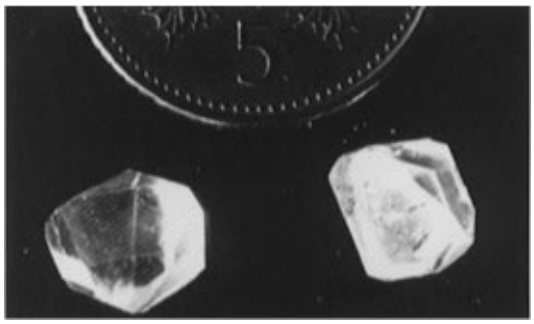

Figure 2. Single crystals grown from pentane using a cooling rate of 0.04 °C h^{-1}. The approximate dimensions of the crystals are 0.6 cm × 0.6 cm × 0.4 cm. The uppermost plane of the left crystal is $(\bar{1}11)$ while for the right it is (010). At the top of the figure is a British 5 pence coin with diameter of about 1.7 cm.

A chloride ISE or a conductivity detection system were utilized to monitor the release of the ionic products H^+ and Cl^- from the reacting interface. For the ISE a silver wire of diameter about 1.6 mm was polished smooth and formed into a silver/silver chloride electrode via an established method.[16] All potentiometic measurements were made with reference to a saturated calomel electrode and were accomplished using a Jenway 3030 pH meter. The ISE was calibrated *in situ* after each experiment by flowing known concentrations of chloride solution through the flow cell. A gradient of ca. −57(±1) mV per decade was usually obtained in the calibration plots in good agreement with the theoretical Nernstian response of −59.6 mV per decade expected at 25 °C. Full details of the conductivity detection system will be described elsewhere.[17] In summary it comprises a pair of 0.4 × 0.4 cm platinum electrodes positioned about 0.9 cm downstream of the reacting surface. The impedance between the two Pt electrodes was measured using a Solarton 1250 frequency response analyzer in conjunction with a Solarton 1286 electrochemical interface (Suhlumberger Electronics Ltd., Farnborough, UK).

A TopoMetrix TMX 2000 atomic force microscope (AFM) and a Hitachi S570 electron microscope were employed to image the surfaces of the solid substrate. A commercial TopoMetrix liquid cell was used for in situ AFM imaging of the reacting crystal surface. Prior to a given AFM experiment the crystal surface was cleaned using pentane. The AFM was operated in repulsive force mode.

Results and Discussion

Preliminary experiments were pursued before undertaking CFC studies in which a 0.7-g pellet pressed from particles in the size range 47−445 μm was allowed to hydrolyze in 20 mL of 0.094 M KNO_3 solution. The chloride concentration was monitored using a silver/silver chloride ISE. The concentration of the chloride ion released was found to increase over a period of up to 5 h. This suggests that the reacting surface remains active during this period.

Attention was then directed to CFC measurements. A series of experiments were conducted in which a solution of 0.094 M KNO_3 was flowed in turn over pressed pellets, fused pellets, and single crystals. In each case a downstream chloride sensitive ISE was used to monitor the hydrolysis. Figure 3 shows representative experimentally measured chloride concentrations for a pressed pellet (36−738 μm) as a function of the solution flow rate. All other samples exhibit a similar trend. It should be noted that the chloride concentration decreases with increasing flow rate because of enhanced convective dilution of the products before they reach the detector.[18]

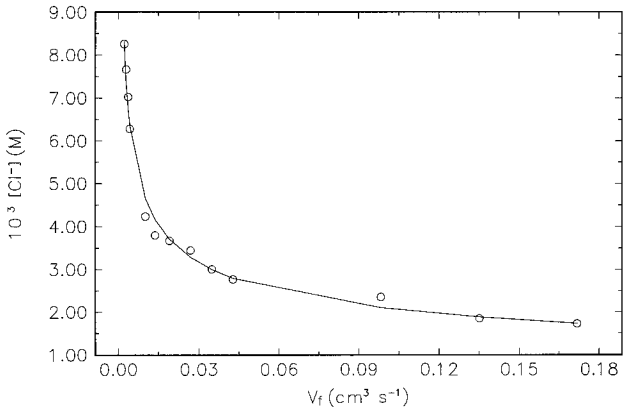

Figure 3. The flow rate dependence of the downstream chloride concentration measured using the ISE for the dissolution of a pressed pellet (36−738 μm particles) into 0.094 M potassium nitrate solution: (○) experimental data and (—) theoretical behavior predicted using the interfacial reaction model and the optimized rate constant shown in Table 2. Cell geometry (see Figure 1): pellet radius, x_p = 9.15 mm; distance between pellet and detector, x_g = 3.11 mm; detector length, x_e = 1.59 mm; and cell depth = 0.102 cm.

The following reaction model was examined to see whether it was consistent with the CFC kinetic data:

$$\mathrm{TPMCl\ (s)} \xrightarrow{k_i} \mathrm{TPM^+(aq) + Cl^-(aq)} \quad (1)$$

$$\mathrm{TPM^+(aq) + H_2O(l)} \xrightarrow{\text{fast}} \mathrm{TPMOH(aq,s) + H^+(aq)} \quad (2)$$

where k_i (mol cm^{-2} s^{-1}) denotes an interfacial reaction rate constant describing the release of triphenylmethyl cations and chloride anions directly from the solid surface into solution. This is assumed to be the rate determining step.

The steady state convective−diffusion equation describing the distribution of the chloride anion within the CFC is

$$\frac{\partial[\mathrm{Cl^-}]}{\partial t} = D_{\mathrm{Cl^-}}\frac{\partial^2[\mathrm{Cl^-}]}{\partial y^2} - v_x\frac{\partial[\mathrm{Cl^-}]}{\partial x} = 0 \quad (3)$$

where the coordinates x and y are defined in Figure 1 and D_{Cl^-}, v_x, and t represent respectively the diffusion coefficient of the chloride anion, the solution flow rate in the x-direction, and time. Values of D_{Cl^-} in aqueous media of different ionic strength at 25 °C have been given by Turq et al.[19]

The theoretical flow rate dependence of the chloride concentration registered by the detector ISE may be computed by solving the above convective-diffusion equation. This requires the specification of appropriate boundary conditions. At the surface of the solid substrate, an interfacial kinetic equation is adopted as the appropriate boundary condition:

$$k_i\ (\mathrm{mol\ cm^{-2}\ s^{-1}}) = -D_{\mathrm{Cl^-}}\frac{\partial[\mathrm{Cl^-}]}{\partial y} \quad (4)$$

Upstream of the solid the chloride concentration is specified as zero while on all boundaries of the cell other than the reacting

(16) Ives, D. J. G.; Janz, G. J. *Reference Electrodes*; Academic Press: New York, 1961.

(17) Tam K. Y.; Larsen, J. P.; Coles, B. A.; Compton, R. G. *J. Electroanal. Chem.* In press.

(18) Convection can be characterized by laminar or turbulent flow. The former describes the solution advancing (through the channel) in separate, non-mixing layers whereas the latter describes a chaotic motion. All experiments conducted in this work were under fully developed laminar flow in which the hydrodynamics is well defined and calculable. As shown in Figure 3, the Cl^- concentration decreases with increasing flow rate as a result of "convective dilution". As the flow rate (convection) increases, the concentration of Cl^- in the zone of the detector decreases since the flux of Cl^- injected from the reacting surface remains essentially fixed.

(19) Turq, P.; Lantela, F.; Chemla, M. *Electrochim. Acta* **1969**, *14*, 1081.

Table 1. The Optimized Interfacial Rate Constants, k_i, for the Hydrolytic Dissolution of TPMCl in $[KNO_3] = 0.094$ M

sample	rate constant[a] (mol cm^{-2} s^{-1})	uncertainty[b] (mol cm^{-2} s^{-1})	RMSD[c] (see eq 6)
pressed (14−90 μm)	2.65×10^{-8}	$\pm 2.42 \times 10^{-10}$	6.47×10^{-4}
pressed (47−445 μm)	2.37×10^{-8}	$\pm 5.84 \times 10^{-10}$	3.63×10^{-4}
pressed (36−738 μm)	1.48×10^{-8}	$\pm 1.88 \times 10^{-9}$	2.23×10^{-4}
fused	2.00×10^{-9}	$\pm 1.51 \times 10^{-10}$	5.33×10^{-5}
crystal ($\bar{1}11$)	3.28×10^{-9}	$\pm 2.65 \times 10^{-10}$	2.83×10^{-5}
crystal (010)	1.94×10^{-9}	$\pm 1.91 \times 10^{-10}$	2.59×10^{-5}
crystal ($\bar{1}10$)	1.22×10^{-9}	$\pm 3.13 \times 10^{-10}$	2.07×10^{-5}

[a] Mean value from at least three separate experiments. [b] Standard deviation from at least three separate experiments. [c] Mean value from at least three separate experiments. RMSD value, obtained from fitting the saturated surface model to the experimental data, as shown in Figure 4, is 2.82×10^{-3}.

surface a no-flux condition is pertinent:

$$0 = D_{Cl^-}\frac{\partial[Cl^-]}{\partial y} \tag{5}$$

Solution of the problem is readily accomplished using the Backward Implicit Finite Difference Method applied in essentially standard form as described elsewhere.[2,3,20,21] No new conceptual or computational problems were encountered in this application and the reader is directed to the literature for the appropriate methodological details. The computations, when made for a known cell geometry and specified D_{Cl^-}, predict the chloride ion concentration throughout the flow cell as a function of flow rate for assumed values of the rate constant k_i. The latter is the only adjustable parameter in the model. The resulting Cl^- concentration profiles may be used to predict the average $[Cl^-]$ over the surface of the potentiometric sensor and hence to predict the dependence of the detector signal on flow rate for different values of k_i. The theoretical data can be related to the experimental results to give a best-fit value of k_i by minimizing the deviation between the theoretical and experimental concentration in a least-squares sense. An error function, root-mean-square-deviation (RMSD) is defined as

$$\mathrm{RMSD} = \sqrt{\frac{\sum_{j=1}^{N}([Cl^-]_{\mathrm{expt},j} - [Cl^-]_{\mathrm{model},j})^2}{N}} \tag{6}$$

where N is the number of data points. The problem then reduces to a nonlinear minimization of RMSD for optimal rate constants. The quasi-Newton method[22] was adopted for this purpose.

The results of the CFC experiments described above were fitted with the proposed heterogeneous reaction model. Figure 3 depicts the theoretical behavior generated using the optimized rate constants which are reported in Table 1. Excellent agreement between experimental data and theoretical prediction is noted over the entire flow rate range. This was in marked contrast with other reaction models that were attempted. In particular poor fits or unsatisfactory interpretations were obtained for models assuming either a saturated surface of TPMCl or a constant flux of TPMCl followed in both cases by homogeneous hydrolysis. As shown in Figure 4, the theoretical product concentration calculated using the estimated solubility of TPMCl[7] (8.64×10^{-8} M) was far below the experimental one regardless of the magnitude of the homogeneous hydrolysis rate constant employed. As for the constant TPMCl flux model, it was found that the theoretical behavior tended toward the proposed heterogeneous reaction model as the homogeneous hydrolysis rate constant was increased to extremely higher values. This observation can be rationalized since as the lifetime of TPMCl(aq) decreases to a minute quantity with respect to the dissolution flux of TPMCl, the model "collapses" into a heterogeneous process in which the reaction can be regarded as occurring effectively at the solid/liquid interface. Moreover, based on the measured hydrolysis reaction flux of about 10^{-8} mol cm^{-2} s^{-1} as reported above (see Table 1) and the solubility of TPMCl ($\approx 10^{-8}$ M), it can be estimated that any reaction layer thickness is not greater than 1 Å. *This implies that the process is indeed authentically interfacial.*

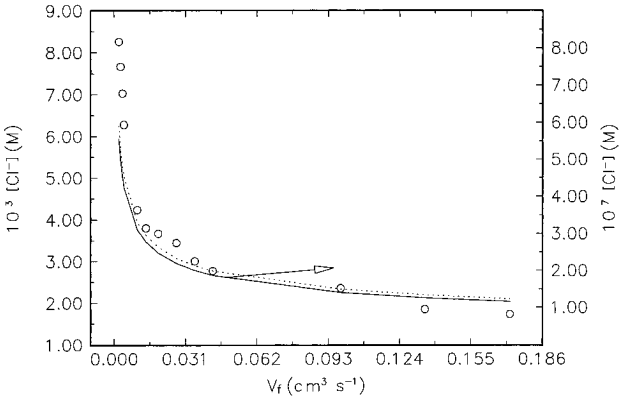

Figure 4. The flow rate dependence of the downstream chloride concentration measured using the ISE for the dissolution of a pressed pellet (36−738 μm particles) into 0.094 M potassium nitrate solution: (○) experimental data and theoretical behavior predicted using the saturated surface model with homogeneous hydrolysis rate constants of 50 s^{-1} (—) and 60 s^{-1} (···). Cell geometry is the same as shown in the caption of Figure 3.

Returning to Table 1 it can be seen that for the pressed pellets the rate constants decrease as the particle size used to form them increases. Also the fused pellet samples show a slower rate of interfacial hydrolysis. These trends probably reflect the surface morphology of the different samples. Scanning electron microscopy (SEM) analysis of the pellet surfaces before dissolution revealed that the pressed pellet surfaces were more porous than that of the fused one. Figures 5 and 6 show respectively the SEM micrographs of a fused pellet and a pressed pellet formed from particles in the size range 36−738 μm from which this difference is readily apparent. The SEM images for the TPMCl particle size ranges of 14−90 and 47−445 μm are qualitatively similar to the 36−738-μm picture; however, the surfaces formed by compressing the materials with wide particle size distributions are appreciably less porous than that from those with narrow distributions. This is probably due to the particles with dissimilar diameters being moulded more easily in a tightly packed manner. Obviously, the larger the surface porosity the larger the apparent interfacial rate constant because of both the increased surface area and the fact that the pores can act as reservoirs of solution containing a high concentration of hydrolysis products.[2,3] Clearly, more structural work is required to definitely establish the effect of surface porosity; this is beyond the aim of the present paper which seeks to establish the authentically interfacial nature of the hydrolysis process.

Table 1 also shows rate constants, k_i, measured for three different crystal faces of single crystals of TPMCl. These were found to obey the sequence:

$$k_i(\bar{1}11) > k_i(010) > k_i(\bar{1}10)$$

(20) Compton, R. G.; Pilkington, M. B. G.; Stearn, G. M. *J. Chem. Soc., Faraday Trans. 1* **1988**, *84*, 2155
(21) Fisher, A. C.; Compton, R. G. *J. Phys Chem.* **1991**, *95*, 7538
(22) *NAG Fortran Library Manual—Mark 13*, Numerical Algorithm Group Ltd.: Oxford, 1988; Vol. 4.

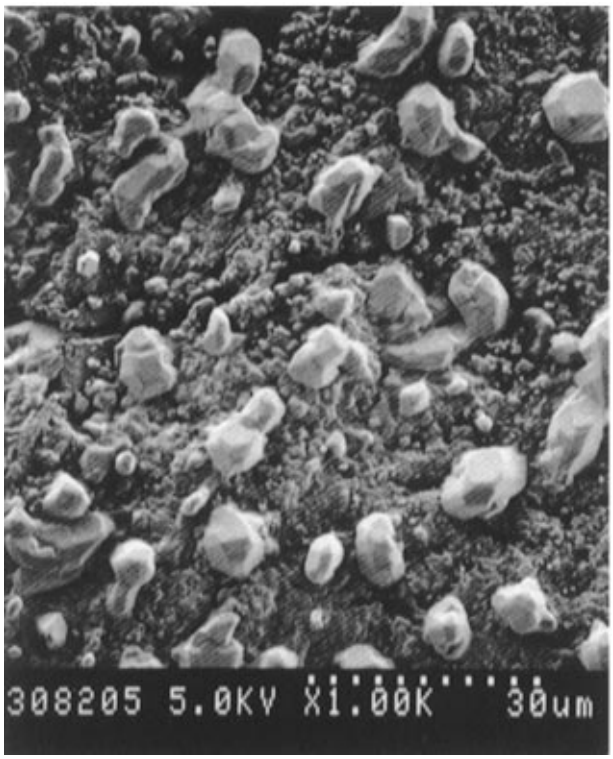

Figure 5. SEM micrograph of a fused pellet before dissolution. The dotted bar represents a distance of 30 μm.

Figure 6. SEM micrograph of a pressed pellet (36−738 μm particles, $D[4,3] = 332.4$ μm) before dissolution. The dotted bar represents a distance of 30 μm.

This trend may be rationalized by assuming the experimental crystal faces approximate to flat surfaces and generating images of each of the three crystal faces studied, using the known crystal structure (as deduced from diffraction) and including molecules located within a depth of 5 Å of the nominal surface. The plots are shown in Figures 7−9. It is possible to distinguish repeat boxes for each of the surfaces. These are in effect 2-dimensional "unit cells" for the surface: each figure shows four of these cells. Inspection of the three figures shows that the density of exposed chlorine atoms changes between the different surfaces.

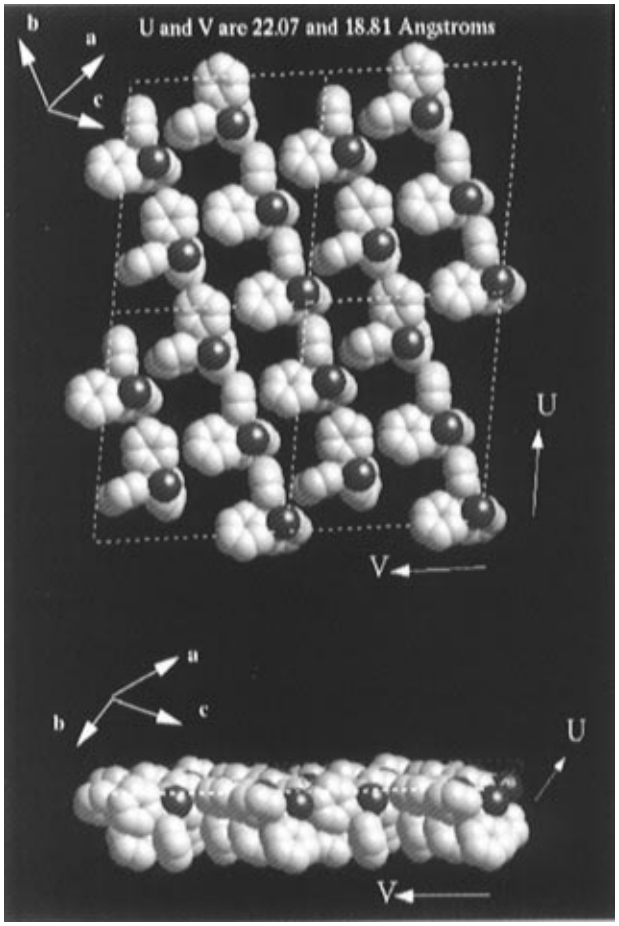

Figure 7. Phase III TPMCl single crystal surface: $(\bar{1}11)$ plane.

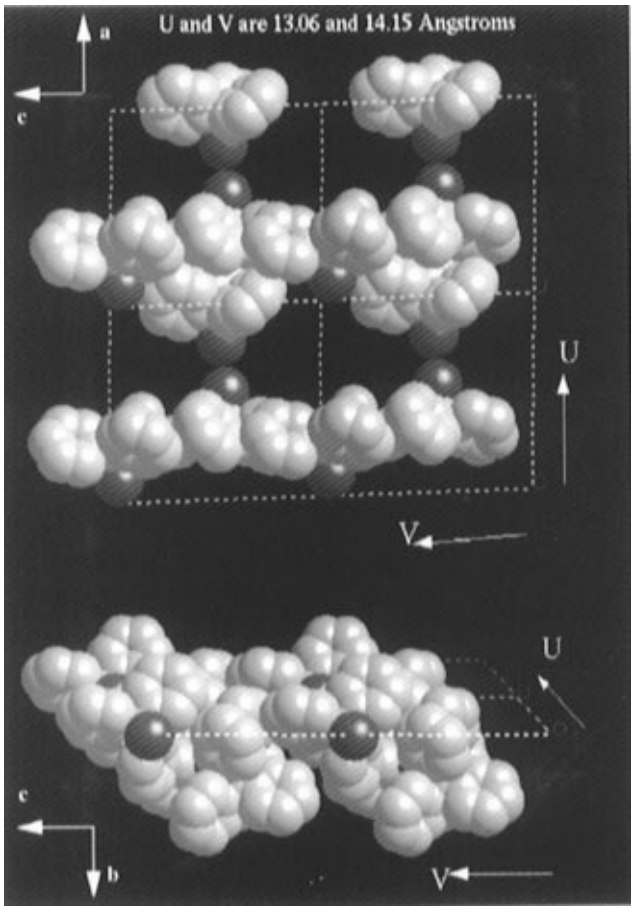

Figure 8. Phase III TPMCl single crystal surface: (010) plane.

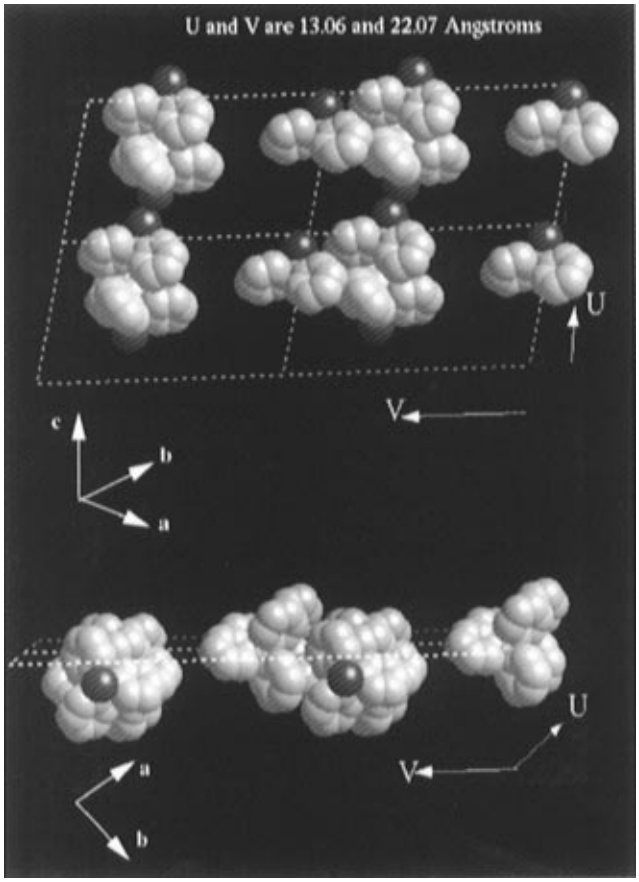

Figure 9. Phase III TPMCl single crystal surface: $(\bar{1}10)$ plane.

Table 2. A Comparison of the Relative Hydrolytic Dissolution Rates to the Density of Chlorine Atoms at the Surface of the Crystal Planes $(\bar{1}11)$, (010), and $(\bar{1}10)$

face	area (Å^2) per reactive Cl atom	relative Cl density in surface	rate constant (mol cm^{-2} s^{-1})	relative reactivities
$(\bar{1}11)$	83	3.5	3.28×10^{-9}	2.7
(010)	184	1.6	1.94×10^{-9}	1.6
$(\bar{1}10)$	288	1.0	1.22×10^{-9}	1.0

Table 3. The Optimized Rate Constants for the Hydrolytic Dissolution of TPMCl Pressed Pellets (47−445-μm Particles) in Aqueous Solutions of Different Ionic Strength

$[KNO_3]$ (M)	rate constant[a] (mol cm^{-2} s^{-1})	uncertainty[b] (mol cm^{-2} s^{-1})
9.40×10^{-2}	2.37×10^{-8}	5.85×10^{-10}
1.89×10^{-2}	1.48×10^{-8}	1.05×10^{-9}
1.51×10^{-3}	1.26×10^{-8}	5.64×10^{-10}
7.54×10^{-4}	1.07×10^{-8}	8.25×10^{-10}

[a] Mean value from at least three separate experiments. [b] Standard deviation from at least three separate experiments.

Figure 7 relates to the $(\bar{1}11)$ surface and contains 5 molecules per repeat box which is of size 22.1 × 18.9 Å. All the chlorine units are pointing up out of this surface so that there is one reactive unit per 82.7 Å^2. Figure 8 shows the (010) surface. The basic repeat unit is 13.1 × 14.1 Å and contains three molecules. Only one is actually on the surface; the other two are buried at 3.5 Å below. There is thus one "surface" chlorine atom every 180.0 Å^2. The $(\bar{1}10)$ surface is shown in Figure 9. This again has three "surface" chlorine atoms per repeat box (22.1 × 13.1 Å). Two of these are about 3 Å below the other which is again located in the surface plane. There is one "surface" chlorine atom every 288.8 Å^2. The molecule(s) at the surface have chlorine atoms which point out of the surface

Figure 10. SEM micrograph of fused pellet after 2 h dissolution in a flow cell (flow rate 4×10^{-2} cm^3 s^{-1}). The dotted bar represents a distance of 30 μm.

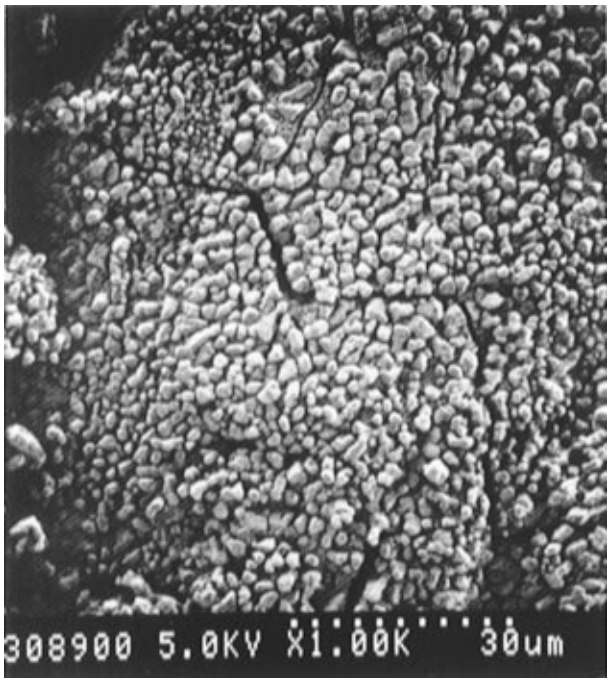

Figure 11. SEM micrograph of pressed pellet (36−738 μm) after 2 h of dissolution in a flow cell (flow rate 4×10^{-2} cm^3 s^{-1}). The dotted bar represents a distance of 30 μm.

in the case of the $(\bar{1}11)$ plane, but in the other two planes the surface molecules have their chlorine atoms lying "in" and along the surface plane.[23]

Table 2 summarizes the density of the chlorine atoms within 5 Å of the surface of the planes $(\bar{1}11)$, (010), and $(\bar{1}10)$. Comparison of these values with the interfacial rate constants measured for the hydrolytic dissolution of TPMCl shows a strong correlation and suggests that the measured differences

(23) It is likely that the $(\bar{1}11)$, (010), and $(\bar{1}10)$ crystal faces will have different solubilities. However, the kinetic experiments presented above indicate that molecules of TPMCl react *without* leaving the solid surface and so we believe solubility contributions are not pertinent to the discussion.

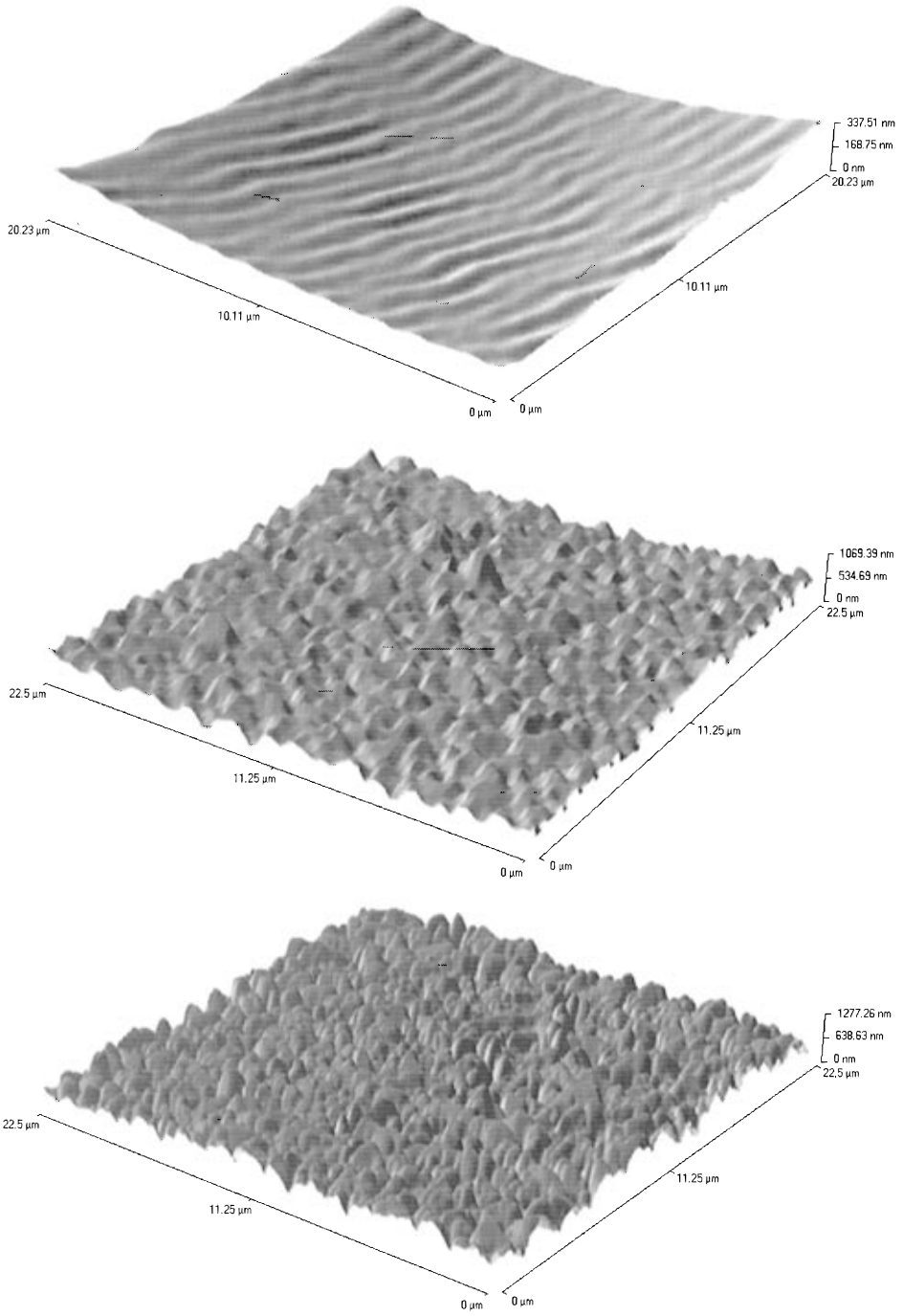

Figure 12. In situ AFM micrographs of the (010) face showing the evolution of an overgrowth layer: (a, top) taken in air; (b, middle) recorded under initially pure water after 2 min of reaction; (c, bottom) recorded under initially pure water after 58 min of reaction.

between the different crystal faces reflect the chlorine atom "availability" in each face.[24] Moreover, the observed correlation provides further evidence to that obtained from the CFC kinetic data that the hydrolytic dissolution is indeed an authentically *heterogeneous* process.

Next CFC dissolution experiments using pressed pellets (47−445-μm particles) were performed in aqueous media of different ionic strength. The chloride ISE sensor was used to study KNO_3 solutions of concentration 0.0940 and 0.0189 M while the conductivity detection system was adopted for 1.50 and 0.754 mM concentrations. In each case the interfacial model of hydrolytic dissolution was found to give an excellent fit to the detector signal/flow rate data. The optimized rate constants for the different concentrations of potassium nitrate are listed in Table 3. The values of k_i increase systematically with ionic strength suggesting, as expected, that the transition state has a greater charge than the reactants.[25] The observed kinetic salt effect suggests that the transition state comprises separated TPM^+ and Cl^- ions.[26]

We next consider the fate of the reaction product TPMOH. CFC experiments with conductivity detection were conducted using pressed pellets (47−445 μm) at a fixed flow rate in the presence of varying amounts of added TPMOH (up to 3.5 ×

(24) The three dimensional unit cells of volume defined by the two-dimensional cells specified in the text and by a depth of one interplanar spacing contain a total of 10 molecules for *each* of the three planes considered. If removal of one surface molecule leads to the dissolution of a unit cell then the dissolution rate will reflect the relative Cl densities given in Table 2.

(25) Gordon J. E. *The Organic Chemistry of Electrolyte Solutions* **1975**, John Wiley & Sons, Inc., New York.

10^{-5} M) to see if, over a period of time, any buildup of TPMOH at the surface might passivate the surface so inhibiting further hydrolytic dissolution. However, after a short initial transient, an essentially constant release of H^+ and Cl^- was observed for periods up to ca 3.5 h, indicating that no significant surface passivation occurs. These CFC experiments are in agreement with the preliminary dissolution work as mentioned above. Next the surfaces of fused and pressed pellets after 2 h of dissolution in the CFC were examined using SEM. Typical images are shown in Figures 10 and 11. Comparison of these with Figures 5 and 6 reveals that a porous overlayer composed of small crystalline solids has become deposited on the pellet surface. We speculate that this is solid TPMOH on account of the estimated low solubility of this material[7] (ca. 10^{-6} M) but note that the similar sized crystals nucleated together. TPMOH is known to self-associate by forming H-bond tetramers which pack in a rather loosely crystalline state.[27,28] The overgrowth generated is rather porous since negligible effects on the dissolution kinetics are observed. Subsequently, the (010) face of a single TPMCl crystal was imaged in real time under water using atomic force microscopy to scrutinize the development of the porous overlayer. In situ micrographs are depicted in Figure 12. Before reaction, the surface was imaged in air (Figure 12a). The presence of terraces with ledge heights ranging from around 2 nm to 30 nm are observed. Once the surface is exposed to water a porous layer forms rapidly: Figure 12b shows a surface after 2 min exposure. Figure 12c indicates that the layer remains almost unchanged after 58 min of exposure. If the developed porous overlayer is contrasted with the fresh surface (Figure 12a), the root-mean-square (RMS) roughness increases from 57−80 nm to 180−240 nm, which corresponds to a three to four times increase. The RMS roughness of the developed overgrowth may be qualitatively correlated to the thickness of the porous layer.

(26) If the kinetic salt effect is assumed to operate on a transition state comprising the separated ions TPM^+ and Cl^- with charges Z_+ and Z_-, respectively, $\log\{k_i(I)\} = \log\{k_i(I = 0)\} + 1.018Z_+Z_-\sqrt{I}$ where we have assumed a temperature of 25 °C. A reasonable straight line is apparent for $\log\{k_i\}$ against $\sqrt{I}$ (see Table 3) and the measured slope has a value of 1.13 which is within 10% of that predicted by the above equation for $Z_+ = -Z_- = 1$.

(27) Weber, E.; Skobridis, K.; Goldberg, I. *J. Chem. Soc., Chem. Commun.* **1989**, 1195.

(28) Ferguson, G.; Gallagher, J. F.; Glidewell, C.; Low, J. N.; Scrimgeour, S. N. *Acta Crystallogr.* **1992**, *C48*, 1272.

Conclusions

The hydrolytic reaction between solid triphenylmethyl chloride and water forming TPMCl takes place at the solid/liquid interface rather than in bulk solution following the prior dissolution of TPMCl. Individual crystal faces appear to react at a rate controlled by the "availability" of exposed chlorine atoms in the reacting surface and kinetic salt effects are consistent with a transition state in which there is essentially full dissociation into the ions TPM^+ and Cl^-. Microscopic studies suggest that a porous overlayer of TPMOH is rapidly formed on the solid surface but contributes negligible resistance to the hydrolysis process.

Acknowledgment. We thank Zeneca Limited for financial support through their Strategic Research Fund Scheme and Dr. Brian Cox for valuable discussions.

JA9529145